

Stochastic reduction for dynamics of reactions with complex formation^{a)}

David J. Zvijac,^{b)} Shaul Mukamel, and John Ross

Department of Chemistry, Massachusetts Institute of Technology, Cambridge, Massachusetts 02139
(Received 28 April 1977)

We present a method for evaluating the distribution of products in chemical reactions which proceed by complex formation. The method consists of separating the degrees of freedom into strong modes, which are correlated directly with the reaction dynamics and weak modes. We then treat the dynamics of the strong modes explicitly and perform a statistical averaging over the weak degrees of freedom. Our final result [Eq. (5)] for the distribution of products is in the form of a product of three matrices whose sizes are determined by the number of relevant strong modes. The first matrix accounts for the preparation of the complex, the second for the energy redistribution within the complex, and the third for the dissociation of the complex. As one possible course of procedure we evaluate the first and third matrices by applying a normal coordinate transformation of the strong modes from reactants to complex and then to products and then use Franck-Condon factors between the strong states of the complex and fragments (reactants and products); the second matrix is evaluated using a step ladder model. We then apply the formulation to the system $F + C_2H_4$ for which deviations from statistical behavior were observed. Nonstatistical behavior may occur in our model from two distinct sources: (1) the Franck-Condon factors which are associated with the dynamics and (2) the finite energy redistribution rate within the complex (relative to the dissociation rate). We discuss the influence of these two effects in $F + C_2H_4$ and conclude that the first one is dominant in this case.

I. INTRODUCTION

The dynamics of reactions of small molecules may be studied by one of many available approaches to the solution of the Schrödinger equation. Thus, exact quantum calculations of molecular scattering can be performed for systems of very few atoms and at low energies (where the number of accessible states is not too large), whereas semiclassical and classical methods are appropriate for higher energies. Statistical theories, on the other hand, have been used successfully in the description of chemical reactions with large molecules over a range of energies. These theories are based on the assumption that due to the large number of states involved in such systems many of the exact dynamical features are being averaged out; thus, it is possible to estimate lifetimes of excited species and branching ratios in chemical reactions by assuming a rapid intramolecular redistribution of energy and then by simply counting states (or measuring the available phase space) without a detailed knowledge about the interactions involved.

Statistical theories are frequently, if not always, applicable to large molecules, provided that we do not ask for too detailed information about the outcome of the reaction. In recent years there have been developed several new experimental techniques which may be used to study the effects of excitation and the intramolecular energy redistribution rates on the decay of excited molecular species and on reactivity.¹⁻⁶ Some of these methods are infrared chemiluminescence,¹ molecular beam studies of radiationless processes,² single vibronic level fluorescence,³ and mass spectroscopic studies.⁴ Such experiments, which provide detailed information about molecular dynamics, may constitute a critical

check on the range of applicability of statistical theories.

In this paper we present a model for the distribution of the internal states in the products of chemical reactions which proceed via complex formation. We aim to account for the deviations of these distributions from purely statistical behavior. Our main physical assumption is that in large molecules there usually are few "strong" degrees of freedom which participate directly and strongly in the reaction dynamics. These are mainly the degrees of freedom associated with the bonds being formed or broken. The remaining "weak" degrees of freedom are assumed to be weakly correlated to the dynamics.

In Sec. II, starting with the tetradic T matrix, we describe the system in terms of a master equation which results from a statistical averaging over the weak states, and whose size is determined by the number of strong states. The final distribution of products is thus expressed as a product of three matrices of manageable size. The first matrix accounts for the formation of the complex, the second describes intramolecular energy redistribution among the states of the complex, whereas the third matrix accounts for the coupling between the complex and the exit channels.

In Sec. III the matrices for the preparation and decay of the complex are evaluated with Franck-Condon (FC) overlap integrals between the fragment and complex states. Recent work on small molecular systems has shown that Franck-Condon overlaps of nuclear wavefunctions give a reasonable picture of vibrational and rotational distributions for reactive collisions.^{7,8} We use here a FC-type approach for the few strong degrees of freedom and a statistical treatment for the rest. The other matrix is evaluated with the aid of a parameter η which describes the ratio of the rate of intramolecular energy redistribution within the complex to the dissocia-

^{a)}Supported in part by Air Force Office of Scientific Research and the National Science Foundation.

^{b)}NSF Energy Related Postdoctoral Fellow.

tion rate. We then apply the model to the reaction of F+ethylene, for which it has been found that the branching between the vibrational states of the product C_2H_3F ,¹ as well as the amount of energy in translation,⁹ differ significantly from statistical predictions.

The present formulation provides a convenient accounting for deviations from statistical behavior in chemical reactions. The simplicity of our method is due to the relatively small number of strong modes which are explicitly incorporated in the dynamics. This leads to a final expression involving relatively small matrices but which includes the main dynamical features. Non-statistical effects enter into our formulation via the dynamics of preparation and decay of the complex (approximated by Franck-Condon factors), and also via the intramolecular relaxation rate of the complex which may be comparable to the dissociation rate.

II. FORMULATION OF THE MASTER EQUATION

Consider the indirect reactive scattering problem



where a complex X is formed in the first step and then decomposes. For this let us introduce the following assumptions: We describe the system in terms of three electronic states (Fig. 1), where a, c, and b refer to the initial, complex, and final state electronic energy surfaces, respectively. Even if the original problem is electronically adiabatic, we can always find a quasi-adiabatic transformation which defines these three surfaces.¹⁰ The Hamiltonian, which includes the electronic and nuclear coordinates, for our system is given by

$$H = H_0 + V, \quad (2)$$

where

$$H_0 = H_0^a + H_0^b + H_0^c \quad (3)$$

and

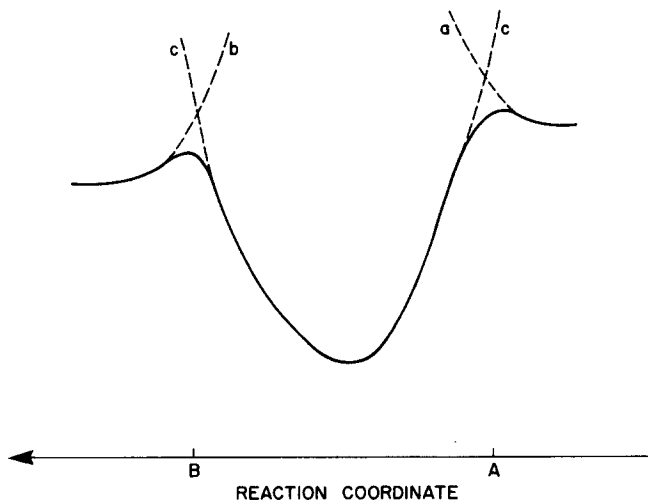


FIG. 1. Schematic of the potential along the reaction coordinate for reactions which proceed via complex formation. Curves (a), (b), and (c) refer to the quasiadiabatic surfaces for the reactant, product, and complex states, respectively.

$$V = V_{ac} + V_{bc} + V_{cc}. \quad (4)$$

Here H_0^i ($i = a, b, c$) denotes the zeroth order Hamiltonian for the i th electronic state. These H_0^i are chosen to our convenience. V_{ac} and V_{bc} are reactive couplings between the incoming and outgoing channels, respectively, and the complex, whereas V_{cc} includes intramolecular couplings in the complex and describes the energy flow within the complex. If we characterize the complex with a harmonic basis set, then V_{cc} includes anharmonicities and describes intramolecular relaxations. Another possibility is to use a local mode description which has been proven recently to be successful in the interpretation of spectra of aromatic molecules.¹¹

We define a few "strong" degrees of freedom which are directly associated with the dynamics. The remaining weak degrees of freedom are assumed to be only mildly correlated with the dynamics. The system has thus three main types of states $|i\alpha\rangle$, $|\lambda\beta\rangle$, and $|f\gamma\rangle$, where i , λ , and f refer to the quantum numbers associated with the strong modes in the a , c , and b states, whereas α , β , and γ refer to the weak degrees of freedom. The states corresponding to the a , c , and b surfaces are orthogonal due to the inclusion of the electronic degrees of freedom. In the Appendix we use the tetradic formalism of Zwanzig and Fano^{12,13} for obtaining a reduced description of a chemical reaction in terms of few degrees of freedom. The tetradic formalism is designed to treat the time evolution of the density matrix of a system in a formal way which is analogous to the ordinary treatment, based on wavefunctions.^{13,14}

The main advantage of this formalism is that it enables us to define projection operators and carry out averagings of the tetradic T matrix \mathcal{T} on the irrelevant weak degrees of freedom. This is due to the fact that the cross sections [Eq. (A10)] are proportional to the matrix elements of \mathcal{T} and not to their square. In contrast with the ordinary T matrix, if we wish to perform any averaging we have first to calculate its elements for all the degrees of freedom, then square, and only afterwards can we average. Our derivation in the Appendix includes a dynamical treatment of the strong modes and a statistical treatment of the weak modes.

We suppose that the correlation time for the interaction between the weak modes (which have only a minor effect on the dynamics) and the strong modes is short compared to the lifetimes of the strong states, so that the weak modes have only an averaged effect. Finally, if the dephasing times of the complex states are much shorter than the decay times so that we can neglect any coherences (off-diagonal elements) and consider only the populations of states, we arrive at our final expression for the reactive cross section

$$\sigma_{i \rightarrow f} \propto \sum_{\lambda, \mu} \Gamma_{f\lambda} G_{\lambda\mu} \Gamma_{\mu i}. \quad (5)$$

Equation (5) describes the scattering event in terms of three matrices; $\Gamma_{\mu i}$ denotes the preparation of the various complex states, $G_{\lambda\mu}$ describes the intramolecular relaxation in the complex, and $\Gamma_{f\lambda}$ describes the dissociation into the exit channels.

Let us now consider each matrix in more detail and attempt some further approximations. For the quantity $\Gamma_{f\lambda}$ we have

$$\Gamma_{f\lambda} = \sum_{\gamma, \beta} |\langle f\gamma | V_{bc} | \lambda\beta \rangle|^2 \rho_\beta / \sum_\beta \rho_\beta, \quad (6)$$

where the sum is over all states γ, β consistent with the relation

$$E = E_f + E_\gamma = E_\lambda + E_\beta, \quad (7)$$

where E is the total energy in the system and ρ_β is the equilibrium probability of populating the weak state β in the complex. We now assume that the coupling element is mainly determined by the strong modes, i. e., the matrix elements $\langle f\gamma | V | \lambda\beta \rangle$ are not very sensitive to the weak quantum numbers γ and β . We thus replace Eq. (6) by

$$\Gamma_{f\lambda} = \langle V_{f\lambda}^2 \rangle \frac{\sum_{\beta} \rho_\beta}{\sum_{\beta} \rho_\beta} = \langle V_{f\lambda}^2 \rangle \rho_f (E - E_f), \quad (8)$$

where $\langle V_{f\lambda}^2 \rangle$ is the coupling between f and λ averaged over all the possible weak states, and $\rho_f(E - E_f)$ is the total density of weak states in the products with energy $E - E_f$. Similarly, we write

$$\Gamma_{\mu i} = \langle V_{\mu i}^2 \rangle \rho_\mu (E - E_\mu). \quad (9)$$

Further, in Eq. (5) we find for the intramolecular relaxation term

$$G_{\lambda\mu} = (\Gamma^{vv} + \Gamma^i + \Gamma^f)_{\lambda\mu}^{-1}. \quad (10)$$

The term Γ^{vv} is due to anharmonicities in the complex [V_{cc} terms in Eq. (4)] which cause vibrational relaxation among the complex states, whereas Γ^i and Γ^f denote coupling between the complex states due to the reactive interactions in the i and f channels, V_{ac} and V_{bc} , respectively. From Eq. (A15) we see that since the diagonal terms $\lambda = \mu$ are of second order in the reactive interaction (V_{ac} , V_{bc}), whereas the offdiagonal terms are of fourth order, it is thus reasonable to write

$$\Gamma_{\lambda\mu}^i = \delta_{\lambda\mu} \sum_i \Gamma_{i\mu} = \delta_{\lambda\mu} \sum_i \langle V_{\mu i}^2 \rangle \rho_i (E - E_i) \quad (11)$$

and

$$\Gamma_{\lambda\mu}^f = \delta_{\lambda\mu} \sum_f \langle V_{\lambda f}^2 \rangle \rho_f (E - E_f). \quad (12)$$

Finally, we note that Eq. (5) is formally equivalent to writing a Pauli master equation for the population of the states of the reaction complex in the following way. For all λ write

$$\frac{dP_\lambda}{dt} = \sum_\mu \Gamma_{\mu\lambda}^{vv} P_\mu - (\Gamma_\lambda^i + \Gamma_\lambda^f) P_\lambda - \Gamma_{\lambda i} \quad (13)$$

The steady state solution is given by

$$(P)_{ss} = \mathbf{G} \Gamma_i, \quad (14)$$

so that the rate of formation of product states is

$$\frac{dP_f}{dt} = \sum_\lambda \Gamma_{f\lambda} (P_\lambda)_{ss} = \Gamma_f \mathbf{G} \Gamma_i, \quad (15)$$

which is identical to Eq. (5). The present formulation,

as detailed in the Appendix, however, enables us to state the approximations made in writing Eq. (15) for our system.

III. MODEL CALCULATIONS AND APPLICATION TO $F + C_2H_4$

To use the formalism of the last section we need to evaluate the elements of the matrices Γ_i and Γ_f and \mathbf{G} . We now proceed in the following steps.

(1) We describe the coupling between the complex and fragment (reactant or product) manifolds by Franck-Condon overlaps γ of the nuclear quasiadiabatic wavefunctions on each of the surfaces. For this purpose we perform a normal mode analysis on the reactant, complex, and product species to determine three sets of normal coordinates.¹⁵ For the products and reactants we carry out the normal mode analysis of each fragment and treat the relative translational degrees of freedom as follows: We fix the reactant (product) fragments at some position and orientation which corresponds to the saddle point of the exit (entrance) barrier. We then write the translational coordinate as a one-dimensional coordinate describing the relative motion of the centers of mass of the fragments.

(2) We define transformation matrices

$$Q^k = \mathbf{C}^k (Q^c - Q^{0k}), \quad k = a, b, \quad (16)$$

between the sets of coordinates.

In Eq. (16) \mathbf{C} is an orthogonal matrix which aligns the two coordinate systems and Q^0 is a vector which describes the displacement of the coordinate systems due to the change in equilibrium geometry of the molecules during the course of the collision.

The transformation matrices \mathbf{C} are a quantitative measure of how the various modes mix in the course of a reaction. As expected intuitively one generally finds that similar modes transform mainly among themselves, i. e., the CH stretching coordinates of a reactant species transform almost entirely to the CH coordinates of a product species. Similarly, heavy atom motion in the carbon skeleton of an organic reactant tends to transform to similar motions of that skeleton in the product. The Q^0 vectors are a measure of the deformation in the equilibrium geometry of the molecule. Thus, during the reaction if the geometry changes near some site in the molecule, the coordinates corresponding to motion near that site will have large Q_i^0 .

(3) We next separate the coordinates of the system into a few strong coordinates and the rest (weak). In general, only a few normal coordinates of the complex are associated with the bonds being formed or broken and will project onto either the reactant or product translational coordinates. These coordinates are taken as the strong modes since they are most directly associated with the dynamics of the reaction.

(4) We write the wavefunction for the complex as a product of harmonic oscillator functions in each of the normal coordinates and the wavefunctions for the fragments as harmonic oscillator functions times a separable

translational wavefunction. We further assume that the $\langle V_{f\lambda}^2 \rangle$ and $\langle V_{i\mu}^2 \rangle$ are proportional to the square of the Franck-Condon factors, i. e.,

$$\begin{aligned} \langle V_{f\lambda}^2 \rangle &\propto \gamma_{\lambda f}^2, \\ \langle V_{i\mu}^2 \rangle &\propto \gamma_{i\mu}^2, \end{aligned} \quad (17)$$

where the FC factors for the strong modes are given by

$$\begin{aligned} \gamma_{\lambda n}^k &= \int d\mathbf{Q}^k \prod_{i=1}^s HO_{\lambda_i}^c(\sqrt{\nu_i^c} Q_i^c) \\ &\times \prod_{j=2}^s HO_{n_j}^k(\sqrt{\nu_j^k} Q_j^k) \chi_{\epsilon}^k(Q_i^k). \end{aligned} \quad (18)$$

Here the ν 's are the vibrational frequencies of the various modes, s is the number of strong modes, and χ_{ϵ}^k is a translational wavefunction for translational energy equal to ϵ .

(5) To evaluate Eq. (18) we must first write an appropriate form for the translational wavefunction. The simplest choice for χ_{ϵ}^k is $\epsilon^{-1/4} \delta(Q_1^k - Q_1^{0k})$, where Q_1^{0k} is the position of the curve crossing of the quasideiabatic surfaces or alternatively the position of the top of the entrance or exit barrier (points A and B in Fig. 1). Alternatively, both the quasideiabatic complex wavefunction and the product translational wavefunction are highly oscillatory so that we can perform a saddle point integration in the translation coordinate. Due to the oscillatory nature of the wavefunctions the major contribution to the integration over the translational coordinate is localized near the curve crossing.

In either of the above cases the translational integral is performed by evaluating a function at a single point. Thus, the analytic evaluation of the FC factors is quite similar to the evaluation of the $\gamma_{\lambda n}$ of R -matrix theory.¹⁶

To evaluate Eq. (18) we rewrite the harmonic oscillator wavefunctions for the complex and fragment systems using the generating function form of the Hermite polynomials. Then, with Eq. (16) we transform all the functions to a single set of orthogonal coordinates. This leaves a multivariate Gaussian integration which can then be performed by standard techniques.

(6) The last thing necessary to evaluate the coupling between the fragments and the complex is an expression for the density of states term $\rho_{\omega}^{\omega}(E_{\omega})$. We use the Whitten-Rabinovitch approximation¹⁷ for the density of vibrational states in the weak modes

$$\rho_{\omega}^{\omega}(E_{\omega}) = (E_{\omega} + a\epsilon_{\omega})^{s-1} / \left[(s-1)! \prod_{i=1}^s \hbar\omega_i \right], \quad (19)$$

where s is the number of weak modes, ϵ_{ω} is the sum of the zero point energies of these modes, ω_i is the frequency of mode i , and a is an empirical parameter dependent on the ω_i , s , and $E_{\omega}/\epsilon_{\omega}$. This counting of states neglects conservation of angular momentum. If angular momentum conservation is an important consideration, then an improved density expression is available in the phase space theory of Light¹⁸ or other similar theories.

The density of states in the weak modes may be written in the form

$$\rho^{\omega}(E - E_f) = \int_0^{E-E_f} d\epsilon \rho_v^{\omega}(\epsilon) \rho_{\text{tr}}(E - E_f - \epsilon), \quad (20)$$

where $\rho_{\text{tr}}(u)$ is the density of translational states with energy u , i. e.,

$$\rho_{\text{tr}}(u) = \sqrt{u}. \quad (20a)$$

The rate of formation of a state λ from reactants is thus given by

$$\Gamma_{\lambda i} = \Gamma_i (\gamma_{\lambda n}^a)^2 \rho_v^{\omega}(E - E_{\lambda}), \quad (21)$$

where Γ_i is a parameter that describes the strength of the coupling between the quasideiabatic manifolds. Similarly, the rate of decay of a complex state λ to a product state f is given by

$$\Gamma_{f\lambda} = \Gamma_d (\gamma_{\lambda f}^b)^2 \rho^{\omega}(E - E_f). \quad (22)$$

(7) Finally, to evaluate the relaxation matrix \mathbf{G} we also need a model for energy redistribution among the states of the complex. In our calculations we use the well known step ladder mechanism for relaxation among coupled harmonic oscillators. The strength of the coupling between the various states is taken to be constant. We have assumed that the transition probability from one strong state λ to another λ' vanishes unless λ and λ' differ only in one quantum number

$$\Gamma_{\lambda\lambda'}^{vv} = \Gamma^{vv}(\lambda - \lambda') = \Gamma_{\text{vr}} \rho_v^{\omega}(E - E_{\lambda'}) \Delta(\lambda, \lambda'), \quad (23)$$

where

$$\Delta(\lambda, \lambda') = \lambda_i + 1 \quad (23a)$$

if $\lambda'_i = \lambda_i + 1$ and all the other quantum numbers do not change,

$$\Delta(\lambda, \lambda') = \lambda_i \quad (23b)$$

if $\lambda'_i = \lambda_i - 1$ and all the other quantum numbers do not change, and $\Delta(\lambda, \lambda') = 0$ otherwise. The diagonal elements of the relaxation matrix are given by

$$\Gamma^{vv}(\lambda - \lambda) = - \sum_{\lambda'} \Gamma^{vv}(\lambda - \lambda'). \quad (24)$$

In Eq. (23) Γ_{vr} gives the time scale for the vibrational relaxation and $\rho_v^{\omega}(E - E_{\lambda'})$ is the density of final states in the transition. The matrix describes relaxation of the strong modes into an equilibrium distribution $\rho_{\lambda}^{\text{eq}}$ in which

$$\rho_{\lambda}^{\text{eq}} = [\rho_v^{\omega}(E - E_{\lambda})] / \sum_{\lambda'} \rho_v^{\omega}(E - E_{\lambda'}). \quad (25)$$

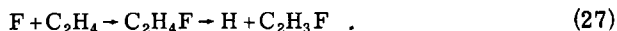
In practice, since we are interested only in product distributions, we neglect the Γ^i term in Eq. (10). This term gives the rate of dissociation of the complex to the original reactants and probably has only a small effect on the product distributions.

(8) After evaluating the three matrices Γ_i , Γ_f and \mathbf{G} we substitute them into Eq. (15) and obtain the final normalized distribution of products

$$P_n = \left(\frac{dP_n}{dt} \right) / \sum_m \frac{dP_m}{dt}, \quad (26)$$

where the dP_m/dt are given by Eq. (15).

The reaction to be studied in detail is



Experiments on this system have been made by Parson and Lee⁹ with crossed molecular beams and by Moehlmann, Gleaves, Hudgens, and McDonald¹ with infrared chemiluminescence techniques. The experimentally observed translational and vibrational energy distributions for this reaction are not consistent with the predictions of statistical theories, despite evidence that the complex has a lifetime of several rotational periods. We analyze this reaction with the model proposed in this paper, proceeding with the steps (1)–(8) just discussed. From the distribution of products [Eq. (26)] we calculate the energy contents of several product modes and the relative translational energy distributions of the product fragments. These results are then compared to the available experimental results, and we point out several reasons for nonstatistical behavior.

For the normal mode analyses we take the results of Shobatake's INDO calculation¹⁹ for the equilibrium geometry of each molecule and use Badger's rule²⁰ for the force constants. From the transformation matrices, which relate all the modes of the complex to the fragments, we find that the initial translational motion of the fluorine atom approaching the center of mass of ethylene transforms very strongly into the CC and CF stretching coordinates of fluoroethylene. On the product side, however, the symmetric and antisymmetric CH₂ stretching coordinates transform very strongly into the product translational motion, namely, hydrogen leaving vinyl fluoride. Thus, we choose to treat explicitly only the four modes (CC, CF, symmetric CH₂, and antisymmetric CH₂ stretches) since these couple strongly to either the reactant or product manifold of states. The frequencies of these strong modes are listed in Table I.

For these strong modes we evaluate the FC factors using Eq. (18). On the reactant side we find that the FC factors are largest for those states of the complex with high excitation in the CC and CF stretching modes and low excitation in the CH modes. Thus, the FC factors indicate that the initial energy of fluorine-ethylene relative motion becomes internal excitation of the CC and CF modes of the complex. On the product side the CH₂ stretching modes of fluoroethylene project strongest onto the product relative translational motion. Consequently, states with high excitation in CH₂ stretch have the largest FC factors on the product side.

The calculations were performed at a total energy of 18 200 cm⁻¹ (52 kcal) above the bottom of the complex well. This is about the average energy at which the experiments were performed. For this total energy 4550 cm⁻¹ (13 kcal) of energy is available for product vibrational and translational energy.

We evaluated the product vibrational distributions for several values of the parameter

$$\eta = \frac{\text{Tr} \Gamma^{vv}}{\text{Tr} \Gamma^f} \propto \frac{\Gamma_{\text{tr}}}{\Gamma_d} \quad (28)$$

where Γ^{vv} and Γ^f were described in Eqs. (23) and (22), respectively. For the sake of calculating the branching

TABLE I. Strong modes and frequencies (in cm⁻¹) for the reactant, complex, and product species of the F+ethylene reaction from the normal mode analysis.

Description	Reactants	Complex	Products
CC stretch	1565	1430	1730
CF stretch		1130	1180
Symmetric CH ₂ stretch	2750	2790	
Antisymmetric CH ₂ stretch	2810	2850	
CH stretch			2810

between the various vibrational channels only the ratio $\Gamma_{\text{tr}}/\Gamma_d$ (and not their absolute values) is important. The parameter η with value equal to zero corresponds to the limit where vibrational relaxation is infinitely slow on the time scale of dissociation of the complex, while η equal to infinity is the limit where relaxation is instantaneous on this time scale.

The energy contents of the strong modes are calculated with the formula

$$E_i = \hbar\omega_i \sum_n n_i P_n \quad (29)$$

where P_n is the probability that the n th channel is populated [Eq. (26)] and n_i are the number of quanta in the i th mode for channel n . The product vibrational state probabilities P_n come directly out of the numerical solution of Eq. (15).

The energy contents of the weak modes are somewhat more complicated to evaluate, since in our stochastic formulation we have lost all information about populations of specific modes and only know the total energy in the weak modes. Consistent with the assumption that weak mode i participates statistically among all the weak modes we have

$$E_i = \hbar\omega_i \sum_n P_n \sum_{m=0}^{m_{\text{max}}} m \rho'(E - E_n - m\hbar\omega_i) \quad (30)$$

where m ranges over the possible number of quanta in mode i (consistent with energy conservation) and $\rho'(E_b)$ is the density of states at energy E_b of the other weak modes, not counting mode i . It can be evaluated in a similar fashion to ρ^ω [Eq. (20)].

The translational energy distribution is given by

$$P_{\text{tr}}(\epsilon) = \sum_n P_n \frac{\rho_v^\omega(E - E_n - \epsilon) \rho_{\text{tr}}(\epsilon)}{\rho^\omega(E - E_n)} \quad (31)$$

where

$$\int d\epsilon P_{\text{tr}}(\epsilon) = 1 \quad (31a)$$

This is equivalent to assuming a statistical partitioning of the energy not in the strong modes among the weak modes and the translational motion as in Eq. (20).

The energy content of several vibrational modes and the ratios between modes are listed in Table II for several values of the parameter η . We see that in the ab-

TABLE II. Energy content (in cm^{-1}) and ratios of energy contents of the CC stretch (1730 cm^{-1}), CF stretch (1180 cm^{-1}), and CH bend (900 cm^{-1}) modes of vinyl fluoride. Shown here are the results for several values of the parameter η as well as the experimental and statistical results.

η	E_{CC}^a	E_{CF}^a	E_{CH}^b	$\frac{E_{CF}}{E_{CH}}$	$\frac{E_{CC}}{E_{CH}}$	$\frac{E_{CC}}{E_{CF}}$
0	865	2306	71	32.9	12.3	0.37
10^{-2}	668	2301	93	24.7	7.2	0.29
1 [†]	621	1546	189	8.2	3.3	0.40
10^{-1}	391	861	295	2.9	1.3	0.44
10	223	502	362	1.39	0.62	0.44
100	171	392	381	1.03	0.45	0.44
∞	142	323	388	0.82	0.36	0.44
Experimental ^c				0.63	0.18	0.29
Statistical ^c				0.85	0.53	0.62

^aFrom Eq. (29).

^cReference 1.

^bFrom Eq. (30).

sence of energy redistribution ($\eta=0$) most of the energy goes into the CC and CF modes. This is what would be expected on intuitive grounds since one can picture that as the fluorine atom attacks ethylene it sets the heavy atom chain in motion. Since energy does not filter out of these initially excited modes due to relaxation, when the complex finally dissociates the CCF modes are still excited.

As η is increased we see a smooth trend of less energy going into CCF modes of products. This effect arises since the relaxation allows energy to transfer from the initially highly excited CCF modes to the initially less excited modes. These lower energy CCF modes of the complex then project onto product modes with less CCF excitation. As the energy relaxes out of the CCF chain we also see a corresponding increase in the energy content of the product bath modes and the CH stretching modes. We make the very important point that even in the $\eta \rightarrow \infty$ limit of instantaneous relaxation in the complex we do not obtain statistical product vibrational dis-

tribution because of our inclusion of the FC factors for the strong modes.

In comparing our results to the experimental results of Moehlmann *et al.* we find best agreement for $\eta = \infty$. Thus, our calculations indicate that energy becomes statistically distributed during the lifetime of the fluoroethylene complex. Nonstatistical product distributions in our interpretation are due to the FC factors which determine the nature of the coupling between complex and product states.

The translational energy distribution corresponding to $\eta = \infty$ is shown as curve A in Fig. 2. The shape of this distribution is quite similar to that given by RRKM-like theories, although somewhat broader. The average translational energy for curve A is 3.6 kcal. This is less than the experimental value of 6.5 kcal (about half the available final energy), but greater than that predicted by statistical theories.

In the above analysis we have neglected entirely the effect of the exit barrier, which is estimated to be 3–4 kcal for this reaction. For translational energies greater than the height of the barrier E_{bar} the barrier probably has only a small effect on the results. For translational energies less than E_{bar} , however, the shape of the barrier strongly affects the translational wavefunctions since they decay inside the barrier.

For a fixed value of the barrier height we now examine how the width of the barrier affects the FC factors. To understand the effects of the exit barrier on the results let us first look at two limiting cases. In the limit that the barrier is narrow the translational wavefunction is nearly the same as that in the absence of a barrier, so that the contribution to the FC factor of the integration over the translational coordinate is nearly the same as if we had neglected the barrier. If the barrier is very wide, the translational wavefunction decays a great deal before it can appreciably overlap with the complex wavefunctions. Thus, the FC factors for low translational energy tend towards zero.

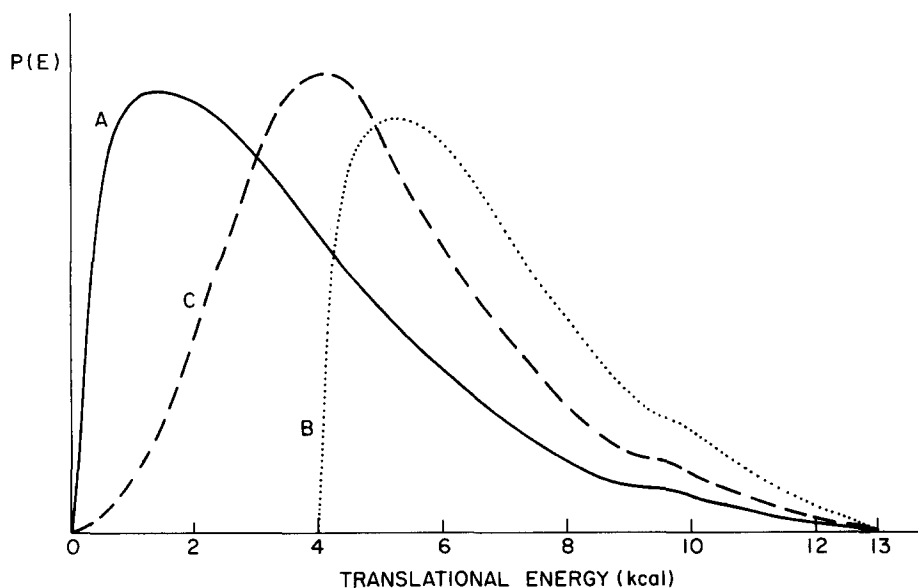


FIG. 2. Relative translational energy distributions calculated from model. (A) Distribution obtained neglecting effects of the exit barrier [$F(\epsilon) = 1$ in Eq. (34)]. (B) Distribution obtained assuming no tunneling through the 4 kcal exit barrier [$F(\epsilon) = \theta(\epsilon - E_{\text{bar}})$, where θ is a step function]. (C) Distribution obtained using value of $b/a = 1$ in Eq. (34).

In actual cases, of course, the FC factors are expected to be between the above limits. Suppose that for $E_t < E_{\text{bar}}$ we take the translational wavefunction to be a delta function at the classical turning point on the dissociative surface. If the repulsive potential is exponential $V = E_{\text{bar}} e^{-aQ_t^h}$, then the energy dependence of the classical turning point is

$$Q_{\text{CTP}}^h = -\frac{1}{a} \ln\left(\frac{E_t}{E_{\text{bar}}}\right). \quad (32)$$

If the translational wavefunction on the complex hypersurface is decaying as $e^{-bQ_t^h}$, then the contribution to the FC factor from the translational integration varies as

$$\text{FC} \propto \left(\frac{E_t}{E_{\text{bar}}}\right)^{b/a}. \quad (33)$$

We can incorporate this effect into our formulation by replacing $\rho_{\text{tr}}(\epsilon)$ in Eqs. (31) and (20) by

$$\rho'_{\text{tr}}(\epsilon) = \rho_{\text{tr}}(\epsilon) F(\epsilon), \quad (34)$$

where

$$F(\epsilon) = \begin{cases} (\epsilon/E_{\text{bar}})^{2b/a}, & \epsilon < E_{\text{bar}}, \\ 1, & \epsilon \geq E_{\text{bar}}, \end{cases} \quad (34a)$$

If we take $F(\epsilon)$ to be zero for $\epsilon < E_{\text{bar}}$, we get the translational energy distribution shown as curve B in Fig. 2. This curve has a threshold at 4 kcal, since we assumed that all the potential energy of the barrier went into translational energy asymptotically as the fragments separated. Curve B has the same general shape as Curve A but $\langle E_t \rangle$ now equals 7.1 kcal, somewhat above the experimental value.

When we take $F(\epsilon) = 0$ for $E_t < E_{\text{bar}}$ the vibrational distributions are altered as well as the translational distributions. These distributions for $\eta = 0$ and ∞ are shown in Table III. In this no tunneling approximation for treating the exit barrier, agreement with experiment regarding the vibrational distributions, and average translational energy is somewhat better than the results shown in Table II.

Neither translation distributions A or B have the same shape as the experimental curve from the beam results of Parson and Lee. Taking a reasonable value of $b/a = 1$ in Eq. (33) leads to curve C in Fig. 2, which shows a closer resemblance to the experimental curve. The choice of $b/a = 1$ corresponds to the barrier being symmetrical such that the slope of the potential surface along the translational coordinate is the same on both the product and complex sides of the saddle point.

TABLE III. Energy content and ratio of energy contents using no tunneling model for the exit barrier [i.e., $F(\epsilon) = 0$ for $\epsilon < E_{\text{bar}}$ in Eq. (34)].

η	E_{CC}	E_{CF}	E_{CH}	$\frac{E_{\text{CF}}}{E_{\text{CH}}}$	$\frac{E_{\text{CC}}}{E_{\text{CH}}}$	$\frac{E_{\text{CC}}}{E_{\text{CF}}}$
0	550	1372	58	23.7	9.5	0.40
∞	81	212	301	0.70	0.27	0.38
Experimental				0.63	0.18	0.29

Curve C rises slowly from a zero energy threshold and has an average translational energy intermediate between the limiting cases A and B. These curves thus demonstrate the qualitative influence of tunneling through the exit barrier on the translational energy distribution.

IV. DISCUSSION

We have developed a method which combines dynamical and stochastic approaches to the analysis of collisions of molecules which lead to reaction through complex formation. Beginning with the tetradic T matrix we derive a master equation for the product vibrational distribution of reactions which proceed through a complex. Dynamical considerations suggest a separation of the degrees of freedom into a set of strong modes, which participate directly in the reaction and are therefore treated explicitly, and weak modes which are treated statistically. This separation is possible when motion along the fragment reaction coordinates, which corresponds to bonds forming and breaking, transforms into only a few modes of the complex. Because of this separation, we can reduce the necessary dynamical calculations to manageable size, determined by the number of strong modes.

The formation and decay of the complex is described by FC factors of wavefunctions on the reactant, complex, and product quasiadiabatic surfaces. The well known step ladder mechanism is used for the vibrational energy redistribution within the complex. We then introduce a parameter η which describes the relative rates of vibrational energy redistribution among the states of the complex vs dissociation of the complex into products.

This model allows us to characterize a wide range of possible systems, from those in which the time scale of vibrational relaxation is much shorter than the time scale of dissociation to those in which it is much longer. In intermediate cases we can see the effects of competition between the two processes.

Even in the limit of fast relaxation, however, the results may be different from those predicted by a fully statistical theory. This is due to the dynamics of the strong modes as shown by nonstatistical FC factors. In the case of fluoroethylene the FC factors seem to be important in determining the vibrational energy ratios. Many systems, of course, are well described by the fully statistical expressions. Such statistical behavior would show up in our results if the FC factors themselves were statistical, i.e., if they showed no trends in magnitude as a function of the quantum numbers. These types of FC factors might arise if, for a fixed fragment configuration, the coordinate transformations were smeared out so that many modes mixed among themselves. Another possible reason is that the relative orientation of fragments leading to preparation and decay of the complex is ill defined, so that the results should be averaged over many different configurations, which may then average out the dynamical effects.

Final state interactions may be included in the present formulation by using the nonreactive quasiadiabatic wavefunctions on the a and b surfaces of Fig. 1 for the

evaluation of the FC factors. Since, however, we can account for the experimental data using the present formulation, we find it unnecessary to include these effects in our calculations. Nonetheless, either a more detailed knowledge of the potential surface or more comprehensive experimental data may make it desirable to consider those effects.

As a final point we consider qualitative trends of our predictions for molecular systems similar to fluoroethylene. We first look at the predictions of our model for the case in which the molecular size increases, all other things being equal. Thus, consider an analogous reaction to fluorine plus ethylene which has the same potential surface features and the same set of strong modes, but has more weak modes. The only difference in our equations for the two cases then is in the density of states terms, since there are more weak modes. We recall that the available vibrational energy in the complex (52 kcal) is considerably larger than in the products (13 kcal including translation) and that the density of states increases strongly with the number of weak modes. Thus, the relaxation terms will be more strongly affected than the dissociation terms. Consequently, for the same ratio of $v-v$ to dissociative coupling strengths (i. e., Γ_{vr}/Γ_d) the corresponding value of η in the case of the larger molecule will be larger than in the ethylene case. Consequently, for the same coupling the vibrational distributions will be closer to the relaxed limit for the larger molecule than for fluoroethylene. This effect is demonstrated in Table IV.

If the coupling ratio Γ_{vr}/Γ_d is independent of energy, as may well be the case, we can apply similar reasoning to predict the trend with increasing total energy. Thus, since the density of states terms for the complex are more sensitive to changes in energy than are those of the products, η will increase with energy. Consequently, the relaxed limit will be approached more quickly as the total energy is increased. This effect has been noticed in studying the ergodic behavior of two coupled oscillators.²¹ For low energy the system is localized in state space, but as the energy is increased the distribution of the system among the states is broadened.

It may be of interest to continue this work by investigating the qualitative features of FC factors for typical systems to determine the types of vibrational distributions expected. This may include the dependence of the

TABLE IV. Energy contents and ratios for a system having the same strong modes as F+ethylene but nine extra weak modes. Assuming a constant coupling ratio (for the vibrational redistribution and dissociation) η is about 43 times larger in this case than for fluoroethylene. Thus, $\eta=0.43$ (4.3) in this table corresponds to $\eta=0.01$ (0.1) in Table II.

η	E_{CC}	E_{CF}	E_{CH}	$\frac{E_{CF}}{E_{CH}}$	$\frac{E_{CC}}{E_{CH}}$	$\frac{E_{CC}}{E_{CF}}$
0	756	2249	69	32.6	11.0	0.34
0.43	221	545	237	2.30	0.93	0.41
4.3	102	245	276	0.89	0.37	0.42
∞	67	166	285	0.58	0.24	0.40

FC factors on structural effects such as bond angles and conjugation of double bonds, as well as masses and frequencies. One might also consider how localized a region about the reaction site must be treated explicitly, i. e., the appropriate choice of strong modes. Finally it may be of interest to apply the formalism to other processes (e. g., isomerization), where one can make simplifications due to the possibility of multiple time scales as was done here.

APPENDIX. DERIVATION OF THE MASTER EQUATION: TETRADIC FORMALISM

The tetradic analogue \tilde{U} of an ordinary operation U is defined by its action on an ordinary operator A as^{12,13}

$$\tilde{U} \cdot A \equiv [U, A] , \quad (\text{A1})$$

which may be written in the form

$$\begin{aligned} (\tilde{U}A)_{ij} &\equiv \sum_{kl} \tilde{U}_{ij,kl} A_{kl} \\ &\equiv \sum_{kl} \langle\langle ij | \tilde{U} | kl \rangle\rangle \langle k | A | l \rangle . \end{aligned} \quad (\text{A2})$$

Comparison of Eqs. (A1) and (A2) results in

$$\tilde{U}_{ij,kl} = U_{ik} \delta_{jl} - U_{ji}^* \delta_{ik} . \quad (\text{A3})$$

Formally we can expand any tetradic operator in the form

$$\tilde{U} = \sum_{ijkl} |ij\rangle\rangle \tilde{U}_{ij,kl} \langle\langle kl | . \quad (\text{A4})$$

Thus, $|ij\rangle\rangle$ denotes a "state" in Liouville space, whereas $\langle\langle kl |$ represents a tetradic operator. The "scalar product" in this space is defined as

$$\langle\langle ij | kl \rangle\rangle = \text{Tr}(|j\rangle \langle i | k\rangle \langle l |) = \delta_{ik} \delta_{jl} , \quad (\text{A5})$$

where $i, j, k,$ and l belong to a complete orthogonal set. We thus see that tetradic operators are naturally defined in terms of four indices. In particular, if $U=H$ (the Hamiltonian of the system), then $\tilde{U}=L$ (the Liouvillian). Also, when H is partitioned into H_0+V we have $L=L_0+V$ where

$$\begin{aligned} L_0 A &= [H_0, A] , \\ V A &= [V, A] . \end{aligned} \quad (\text{A6})$$

The tetradic S matrix is defined as the transformation between the density matrices of the system before and after the collision, i. e.,

$$\rho_{kl}(+\infty) = S_{kl,ij} \rho_{ij}(-\infty) . \quad (\text{A7})$$

We introduce the tetradic T matrix

$$\mathcal{T}(\omega) = V + V G(\omega) V , \quad (\text{A8})$$

where

$$G(\omega) = (\omega - L + i\epsilon)^{-1} . \quad (\text{A9})$$

V is defined in Eq. (A6) and $H=H_0+V$ is the appropriate partitioning of H for a given scattering problem. We note the formal analogy of Eqs. (A7)–(A9) with the ordinary (dyadic) formalism, the difference being that each operator U is now a commutator. Ordinary cross sections are given by

$$\sigma_{ba}(E_a) = i T_{bb,aa}(0) F_a^{-1} = 2\pi |T_{ba}(E_a)|^2 \delta(E_b - E_a), \quad (\text{A10})$$

where F_a is the incoming flux in the $|a\rangle$ channel.

We next consider the scattering problem discussed in Sec. II and define the following tetradic projections:

$$\begin{aligned} P_a &= \sum_{\substack{i\alpha, \\ i'\alpha'}} |i\alpha, i'\alpha'\rangle \langle\langle i\alpha, i'\alpha' |, \\ P_b &= \sum_{\substack{f\gamma, \\ f'\gamma'}} |f\gamma, f'\gamma'\rangle \langle\langle f\gamma, f'\gamma' |, \\ P_c &= \sum_{\substack{\lambda\beta, \\ \mu\beta'}} |\lambda\beta, \mu\beta'\rangle \langle\langle \lambda\beta, \mu\beta' |, \end{aligned} \quad (\text{A11})$$

which span our total Liouville space, i. e.,

$$P_a + P_b + P_c = 1. \quad (\text{A12})$$

We segregate the Liouville space into a space P including the complex states and $Q = 1 - P$, i. e.,

$$\begin{aligned} P &= P_c, \\ Q &= 1 - P = P_a + P_b. \end{aligned} \quad (\text{A13})$$

We make use of a well known result of scattering theory to write^{12,13}

$$Q T Q = Q R Q + Q R P G P R Q, \quad (\text{A14})$$

where

$$R = \mathcal{U} + \mathcal{U} Q (\omega - Q L Q)^{-1} Q \mathcal{U} \quad (\text{A15})$$

and

$$P G P = (\omega - L_0 - P R P)^{-1}, \quad (\text{A16})$$

and \mathcal{U} is the tetradic analogue of V .

The first term in Eq. (A14) describes a direct coupling between reactants and products and is assumed to vanish in our model of a complex reaction. The second term, however, describes a reaction proceeding via the complex. We introduce the following approximations:

(1) R is evaluated to second order in \mathcal{U} , i. e.,

$$R \cong \mathcal{U} + \mathcal{U} Q (\omega - L_0)^{-1} Q \mathcal{U}. \quad (\text{A17})$$

(2) We define a Zwanzig projection¹²

$$C = \rho_\alpha \text{Tr}_\alpha, \quad (\text{A18})$$

which performs the trace over the weak modes. ρ_α in Eq. (A18) denotes the density matrix for the weak states.

The cross section $\sigma_{a \rightarrow c}$ requires thus the projection $Q C T Q C$. If the correlation time for the interaction between the weak and strong modes is short compared to the lifetimes of the strong states, as might be the case if the density of weak states is large enough, then we can write¹²⁻¹⁴

$$C Q T C Q \cong C Q R P C G P C R Q C, \quad (\text{A19})$$

and the reactive scattering cross section may be explicitly written in the form

$$\begin{aligned} \sigma_{i \rightarrow f} &\propto \sum_{\alpha\gamma} \rho_\alpha \langle\langle f\gamma, f\gamma | Q C T C Q | i\alpha, i\alpha \rangle\rangle \\ &\propto \sum_{\substack{\lambda\lambda', \\ \mu\mu'}} \bar{R}_{ff,\lambda\lambda'} \bar{G}_{\lambda\lambda',\mu\mu'} \bar{R}_{\mu\mu',ii}, \end{aligned} \quad (\text{A20})$$

where the operators \bar{R} and \bar{G} are given by

$$\begin{aligned} \langle\langle ab | \bar{R}(\omega) | cd \rangle\rangle &= \sum_\alpha \rho_\alpha \left[\delta_{bd} \sum_{kb} U_{\alpha b}^{ak} U_{\alpha a}^{kc} (\omega - \epsilon_{kb} - \omega_{b\alpha} + i\eta)^{-1} + \delta_{ac} \sum_{kb} U_{\alpha a}^{kb} U_{\alpha b}^{dk} (\omega - \epsilon_{ak} - \omega_{a\alpha} + i\eta)^{-1} \right. \\ &\quad \left. - \sum_0 U_{\alpha a}^{ac} U_{\alpha b}^{db} (\omega - \epsilon_{cb} - \omega_{a\alpha} + i\eta)^{-1} - \sum_0 U_{\alpha b}^{db} U_{\alpha a}^{ac} (\omega - \epsilon_{ad} - \omega_{b\alpha} + i\eta)^{-1} \right], \end{aligned} \quad (\text{A21})$$

where

$$\begin{aligned} U_{\alpha\beta}^{ab} &\equiv \langle b\beta | V | a\alpha \rangle, \\ \epsilon_{ab} &= E_a - E_b \quad (\text{for the strong modes}), \\ \omega_{\alpha\beta} &= E_\alpha - E_\beta \quad (\text{for the weak modes}), \end{aligned} \quad (\text{A22})$$

and

$$\bar{G}_{ab,cd} = (\omega - \omega_{a\alpha} \delta_{ac} \delta_{bd} - \bar{R}_{ab,cd})^{-1}.$$

We invoke our final approximation which amounts to neglecting the coherences in the complex and considering only populations, i. e., we write

$$\sigma_{i \rightarrow f} \propto \sum_{\lambda,\mu} \bar{R}_{ff,\lambda\lambda'} \bar{G}_{\lambda\lambda',\mu\mu'} \bar{R}_{\mu\mu',ii}. \quad (\text{A23})$$

Due to the large number of degrees of freedom involved we expect to have cancellations in the $\bar{R}_{ff,\lambda\lambda'}$ and $\bar{R}_{\mu\mu',ii}$ terms for $\lambda \neq \lambda'$, $\mu \neq \mu'$ because of the appearance of

many terms with various phases. In addition, $R_{\lambda\lambda',\mu\mu'}$, which appears in the denominator of $G_{\lambda\lambda',\mu\mu'}$, is expected to be much larger for $\lambda \neq \lambda'$, $\mu \neq \mu'$ since dephasing times are expected to be much shorter than the decays of populations. As a result the dominant contribution to the sum [Eq. (A23)] comes from the diagonal terms $\lambda = \lambda'$, $\mu = \mu'$. We then have our final expression:

$$\sigma_{i \rightarrow f} \propto \sum_{\lambda\mu} \Gamma_{f\lambda} G_{\lambda\mu} \Gamma_{\mu i}, \quad (\text{A24})$$

where

$$\begin{aligned} \Gamma_{f\lambda} &= \bar{R}_{ff,\lambda\lambda} \\ \Gamma_{\mu i} &= \bar{R}_{\mu\mu,ii}, \end{aligned} \quad (\text{A25})$$

and

$$G_{\lambda\mu} = \bar{G}_{\lambda\lambda,\mu\mu}.$$

- ¹J. G. Moehlmann, J. T. Gleaves, J. W. Hudgens, and J. D. McDonald, *J. Chem. Phys.* **60**, 2040 (1974).
- ²R. K. Sander, B. Solp, and R. N. Zare, *J. Chem. Phys.* **64**, 1242 (1976).
- ³M. H. Hui and S. A. Rice, *J. Chem. Phys.* **61**, 833 (1974).
- ⁴A. Lee, R. LeRoy, F. Herman, R. Wolfgang, and J. C. Tully, *Chem. Phys. Lett.* **12**, 569 (1972).
- ⁵S. Nordholm and S. A. Rice, *J. Chem. Phys.* **62**, 157 (1974); W. M. Gelbart, S. A. Rice, and K. F. Freed, *J. Chem. Phys.* **57**, 4699 (1972); K. G. Kay, *J. Chem. Phys.* **61**, 5205 (1974).
- ⁶J. D. McDonald and R. A. Marcus, *J. Chem. Phys.* **65**, 2180 (1976).
- ⁷G. C. Schatz and J. Ross, *J. Chem. Phys.* **66**, 1021, 1037 (1977).
- ⁸M. Berry, *Chem. Phys. Lett.* **27**, 73 (1974).
- ⁹J. M. Parson and Y. T. Lee, *J. Chem. Phys.* **56**, 4658 (1972).
- ¹⁰S. Mukamel and J. Ross, *J. Chem. Phys.* **66**, 3759 (1977); T. F. George and J. Ross, *J. Chem. Phys.* **55**, 3851 (1971); T. F. George and J. Ross, *Ann. Rev. Phys. Chem.* **24**, 263 (1973).
- ¹¹R. L. Swofford, M. E. Long, and A. C. Albrecht, *J. Chem. Phys.* **65**, 179 (1977).
- ¹²(a) R. Zwanzig, *Lectures in Theoretical Physics* (Interscience, New York, 1960), Vol. 3; (b) U. Fano, *Phys. Rev.* **131**, 259 (1963); (c) A. G. Redfield in *Advances in Magnetic Resonance*, edited by J. S. Waugh (Academic, New York, 1965), Vol. I.
- ¹³A. Ben-Reuven, *Adv. Chem. Phys.* **33**, 235 (1975).
- ¹⁴A. Ben-Reuven and S. Mukamel, *J. Phys. A* **8**, 1313 (1975).
- ¹⁵E. B. Wilson, J. C. Decius, and P. C. Cross, *Molecular Vibrations* (McGraw-Hill, New York, 1955).
- ¹⁶D. J. Zvijac and J. Light, *Chem. Phys.* **21**, 411 (1977).
- ¹⁷G. Z. Whitten and B. S. Rabinovitch, *J. Chem. Phys.* **38**, 2466 (1963).
- ¹⁸J. C. Light, *Discuss. Faraday Soc.* **44**, 14 (1967).
- ¹⁹K. Shobatake, Ph.D. thesis, University of Chicago (1974).
- ²⁰See H. S. Johnston, *Gas Phase Reaction Rate Theory* (Ronald, New York, 1966), p. 72 ff.
- ²¹K. S. J. Nordholm and S. A. Rice, *J. Chem. Phys.* **61**, 203 (1974).